

# Exclusive double diffractive Higgs boson production at LHC

V.A. Petrov, R.A. Ryutin\*

Institute for High Energy Physics, Division of Theoretical Physics, 142281, Protvino, Russia

Received: 5 November 2003 / Revised version: 16 April 2004 /  
 Published online: 30 July 2004 – © Springer-Verlag / Società Italiana di Fisica 2004

**Abstract.** Exclusive double diffractive (EDD) Higgs boson production is analyzed in the framework of the Regge-eikonal approach. Total and differential cross-sections for the process  $p + p \rightarrow p + H + p$  are calculated. Experimental possibilities to find the Higgs boson at LHC are discussed.

## 1 Introduction

LHC collaborations aimed at working in the low (TOTEM)- and high (CMS)- $p_T$  regimes related to typical undulatory (diffractive) and corpuscular (point-like) behaviors of the corresponding cross-sections may offer a very exciting possibility to observe an interplay of both regimes [1]. In theory the “hard part” can be (hopefully) treated with perturbative methods whilst the “soft” one is definitely non-perturbative.

Below we give an example of such an interplay: exclusive Higgs boson production by diffractively scattered protons, i.e. the process  $p + p \rightarrow p + H + p$ , where  $+$  means also a rapidity gap. There are still big differences in the predictions of different authors (see [2] and references therein). Nevertheless, some of them are reconciled by introducing suppressing factors, as will be seen below. In the present paper we will calculate the cross-section of the process in the improved Regge-eikonal model [3].

This process is related to the dominant amplitude of exclusive two-gluon production. The driving mechanism of the diffractive processes is the pomeron. Data on the total cross-sections unambiguously demand a pomeron with larger-than-one intercept, from which follows the need in “unitarization”.

As will be seen below the detection of the Higgs boson (in the  $b\bar{b}$  mode) at LHC in the double diffractive regime looks fairly well possible.

## 2 Calculations

In Figs. 1 and 2 we illustrate in detail the process  $p + p \rightarrow p + H + p$ . Off-shell proton-gluon amplitudes in Fig. 2 are treated by the method developed in [3], which is based on the extension of the Regge-eikonal approach, and successfully used for the description of the HERA data [4].

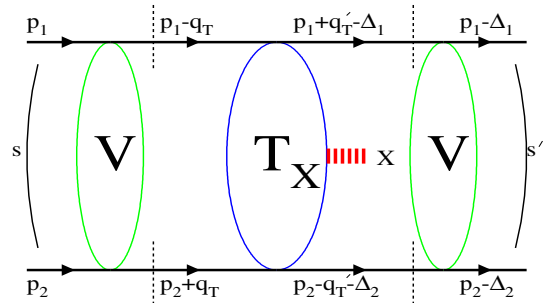


Fig. 1. Unitarization of the process  $p + p \rightarrow p + X + p$

The amplitude of the process  $p + p \rightarrow p + H + p$  consists of two parts (see Fig. 2). The “hard” part  $F$  is the usual gluon-gluon fusion process calculated in the standard model [5]. “Soft” amplitudes  $T_{1,2}$  are obtained in the Regge-eikonal approach.

We use the following kinematics, which corresponds to the double Regge limit. It is convenient to use light-cone components  $(+, -, \perp)$ . The components of the momenta of the hadrons in Fig. 2 are

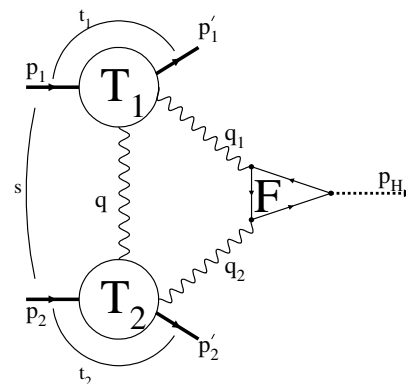


Fig. 2. The “bare” amplitude of the process  $p + p \rightarrow p + H + p$

\* Send offprint requests to: R.A. Ryutin  
 Correspondence to: ryutin@th1.ihep.su

$$\begin{aligned}
p_1 &= \left( \sqrt{\frac{s}{2}}, \frac{m^2}{\sqrt{2s}}, \mathbf{0} \right), \\
p_2 &= \left( \frac{m^2}{\sqrt{2s}}, \sqrt{\frac{s}{2}}, \mathbf{0} \right), \\
p'_1 &= \left( (1 - \xi_1) \sqrt{\frac{s}{2}}, \frac{\Delta_1^2 + m^2}{(1 - \xi_1) \sqrt{2s}}, -\Delta_1 \right), \\
p'_2 &= \left( \frac{\Delta_2^2 + m^2}{(1 - \xi_2) \sqrt{2s}}, (1 - \xi_2) \sqrt{\frac{s}{2}}, -\Delta_2 \right), \\
q &= (q_+, q_-, \mathbf{q}), \\
q_1 &= q + p_1 - p'_1 = q + \Delta_1, \\
q_2 &= -q + p_2 - p'_2 = -q + \Delta_2.
\end{aligned} \tag{1}$$

The  $\xi_{1,2}$  are the fractions of protons momenta carried by gluons. For two-dimensional transverse vectors we use boldface type. From the above notation we can obtain the relations

$$\begin{aligned}
t_{1,2} &= \Delta_{1,2}^2 \simeq -\frac{\Delta_{1,2}^2(1 + \xi_{1,2}) + \xi_{1,2}^2 m^2}{1 - \xi_{1,2}} \\
&\simeq -\Delta_{1,2}^2, \quad \xi_{1,2} \rightarrow 0, \\
\cos \phi_0 &= \frac{\Delta_1 \Delta_2}{|\Delta_1| |\Delta_2|}, \\
M_H^2 &\simeq \xi_1 \xi_2 s + t_1 + t_2 - 2\sqrt{t_1 t_2} \cos \phi_0, \\
(p_1 + q)^2 &\simeq m^2 + q^2 + \sqrt{2s} q_- = s_1, \\
(p_2 - q)^2 &\simeq m^2 + q^2 - \sqrt{2s} q_+ = s_2.
\end{aligned} \tag{2}$$

The physical region of diffractive events with two rapidity gaps is defined by the following kinematical cuts:

$$0.01 \text{ GeV}^2 \leq |t_{1,2}| \leq 1 \text{ GeV}^2. \tag{3}$$

$$\xi_{\min} \simeq \frac{M_H^2}{s \xi_{\max}} \leq \xi_{1,2} \leq \xi_{\max} = 0.1, \tag{4}$$

$$(\sqrt{-t_1} - \sqrt{-t_2})^2 \leq \kappa \leq (\sqrt{-t_1} + \sqrt{-t_2})^2, \tag{5}$$

$$\kappa = \xi_1 \xi_2 s - M_H^2 \ll M_H^2.$$

The discussion on the choice of the cuts (3)–(5) for diffractive events and references to other authors have been given in [6,7]. Whereas large rapidity gaps are produced for  $\xi_{1,2} \rightarrow 0$ , heavy particle production requires that neither  $\xi_1$  nor  $\xi_2$  be too close to zero. We assume  $\xi_{1,2} < 0.1$  since the cross-sections then become mainly diffractive [8]. The relations in terms of  $y_{1,2}$  and  $y_H$  (hadron and Higgs boson rapidities, respectively) take the form

$$\begin{aligned}
\xi_{1,2} &\simeq \frac{M_H}{\sqrt{s}} e^{\pm y_H}, \\
|y_H| &\leq y_0 = \ln \left( \frac{\sqrt{s} \xi_{\max}}{M_H} \right), \\
y_0 &\simeq 2.5 \text{ for } \sqrt{s} = 14 \text{ TeV}, \quad M_H = 115 \text{ GeV}, \\
|y_{1,2}| &= \frac{1}{2} \ln \frac{(1 - \xi_{1,2})^2 s}{m^2 - t_{1,2}} \geq 9.
\end{aligned} \tag{6}$$

The calculation of the amplitude is based on the non-factorized scheme. The contribution of the diagram de-

picted in Fig.2 is obtained by integrating over all internal loop momenta. It was shown in [7] that the leading contribution arises from the region of the integration where the momentum  $q$  is ‘‘Glauber-like’’, i.e. of the order  $(k_+ m^2 / \sqrt{s}, k_- m^2 / \sqrt{s}, \mathbf{k} m)$ , where the  $k$ 's are of the order 1. A detailed consideration of the loop integral like

$$\int \frac{d^4 q}{(2\pi)^4} \frac{f(q, p_1, p_2, \Delta_1, \Delta_2)}{(q^2 + i0)(q_1^2 + i0)(q_2^2 + i0)}, \tag{7}$$

shows that the main contribution comes from the poles

$$\begin{aligned}
q_1^2 &= \sqrt{2s} \xi_1 q_- - \mathbf{q}_1^2 = 0, \\
q_2^2 &= -\sqrt{2s} \xi_2 q_+ - \mathbf{q}_2^2 = 0.
\end{aligned}$$

In this case

$$q = \left( -\frac{\mathbf{q}_2^2}{\xi_2 \sqrt{2s}}, \frac{\mathbf{q}_1^2}{\xi_1 \sqrt{2s}}, \mathbf{q} \right), \tag{8}$$

where

$$\begin{aligned}
\mathbf{q}_1^2 &= \mathbf{q}^2 + \Delta_1^2 + 2|\mathbf{q}| |\Delta_1| \cos \left( \phi + \frac{\phi_0}{2} \right), \\
\mathbf{q}_2^2 &= \mathbf{q}^2 + \Delta_2^2 - 2|\mathbf{q}| |\Delta_2| \cos \left( \phi - \frac{\phi_0}{2} \right).
\end{aligned}$$

In this region  $|q^2/M_H^2| \ll 1$ , and for the  $ggH$  vertex  $F^{\mu\nu}$  in the first order of the strong coupling we have the usual [5] expression

$$F^{\mu\nu} \simeq \left( g^{\mu\nu} - \frac{2q_2^\mu q_1^\nu}{M_H^2} \right) F_{gg \rightarrow H}, \tag{9}$$

$$F_{gg \rightarrow H} = M_H^2 \frac{\alpha_s}{2\pi} \sqrt{\frac{G_F}{\sqrt{2}}} f(\eta), \tag{10}$$

$$\begin{aligned}
f(\eta) &= \frac{1}{\eta} \left\{ 1 + \frac{1}{2} \left( 1 - \frac{1}{\eta} \right) \left[ \text{Li}_2 \left( \frac{2}{1 - \sqrt{1 - \frac{1}{\eta} - i0}} \right) \right. \right. \\
&\quad \left. \left. + \text{Li}_2 \left( \frac{2}{1 + \sqrt{1 - \frac{1}{\eta} + i0}} \right) \right] \right\},
\end{aligned}$$

where  $\eta = M_H^2/4m_t^2$ , and  $G_F$  is the Fermi constant. The NLO  $K$ -factor of 1.5 for the  $gg \rightarrow H$  process is included to the final answer.

Taking the general form for  $T$ -amplitudes that satisfy the identities

$$q^\alpha T_{\mu\alpha}^D = 0, \quad q_i^\mu T_{\mu\alpha}^D = 0, \tag{11}$$

and neglecting terms of the order  $o(\xi_i)$ , the following expression is found at  $|t_i| \leq 1 \text{ GeV}^2$ :

$$\begin{aligned}
T_{\mu\alpha}^D(p, q, q_i) &= \left( G_{\mu\alpha} - \frac{P_{\mu}^{q_i} P_{\alpha}^q}{P_{q_i} P_q} \right) T_{gp \rightarrow gp}^D(s_i, t_i, qq_i) G_{\mu\alpha} \\
&= g_{\mu\nu} - \frac{q_{i,\mu} q_{\alpha}}{qq_i},
\end{aligned}$$

$$\begin{aligned}
P_\mu^{q_i} &= p_\mu - \frac{pq_i}{qq_i} q_\mu, \\
P_\alpha^q &= p_\alpha - \frac{pq}{qq_i} q_{i,\alpha}.
\end{aligned} \tag{12}$$

For  $T_{gp \rightarrow gp}^D$  we use the Regge-eikonal approach [3,9]. At small  $t_i$  it takes the form of the Born approximation, i.e. the Regge factor:

$$\begin{aligned}
&T_{gp \rightarrow gp}^D(s_i, t_i, qq_i) \\
&= c_{gp} \left( e^{-i\frac{\pi}{2}} \frac{s_i - qq_i - m^2}{s_0 - qq_i - m^2} \right)^{\alpha_P(t_i)} e^{b_0 t_i}, \tag{13}
\end{aligned}$$

$$b_0 = \frac{1}{4} \left( \frac{r_{pp}^2}{2} + r_{gp}^2 \right), \tag{14}$$

where

$$\begin{aligned}
\alpha_P(0) &= 1.203, \quad \alpha'_P(0) = 0.094 \text{ GeV}^{-2}, \\
r_{pp}^2 &= 2.477 \text{ GeV}^{-2}
\end{aligned} \tag{15}$$

are found in [9]. The parameters

$$c_{gp} \simeq 3.5, \quad r_{gp}^2 = 2.54 \text{ GeV}^{-2}, \tag{16}$$

are defined from fitting [10] the HERA data on  $J/\Psi$  photo-production, which will be published elsewhere. It is found that the Born term corresponding to the ‘‘hard’’ pomeron with parameters (15) of the trajectory gives the main contribution to the amplitude. The upper bound for the constant  $c_{gp}^{up} \simeq 2.3$  (3.3) can also be estimated from the exclusive double diffractive di-jet production at Tevatron, if we take CDF cuts and the upper limit for the exclusive total di-jet cross-section [11]. The effective value  $c_{gp} = 2.3$  corresponds to the case when the Sudakov suppression factor is absorbed into the constant, and  $c_{gp} = 3.3$  is obtained when explicitly taking into account this factor.

The full amplitude for Higgs boson production looks as follows:

$$\begin{aligned}
&T_{pp \rightarrow pHp} \simeq \\
&\int \frac{d^4 q}{(2\pi)^4} \frac{8F^{\mu\nu}(q_1, q_2) T_{\mu\alpha}^D(p_1, q, q_1) T_{\nu\alpha}^D(p_2, -q, q_2)}{(q^2 + i0)(q_1^2 + i0)(q_2^2 + i0)}. \tag{17}
\end{aligned}$$

The factor 8 arises from the color index contraction. Let

$$l^2 = -q^2 \simeq \mathbf{q}^2, \quad y_H = \langle y_H \rangle = 0,$$

and contract all the tensor indices; then the integral (17) takes the form

$$\begin{aligned}
&T_{pp \rightarrow pHp} \\
&\simeq c_{gp}^2 e^{b(t_1+t_2)} \frac{\pi}{(2\pi)^2} \left( -\frac{s}{M_H^2} \right)^{\alpha_P(0)} \cdot 8F_{gg \rightarrow H} \cdot I, \tag{18}
\end{aligned}$$

$$b = \alpha'_P(0) \ln \left( \frac{\sqrt{s}}{M_H} \right) + b_0, \tag{19}$$

$$I \simeq \int_0^{M_H^2} \frac{dl^2}{l^4} \left( \frac{l^2}{s_0 - m^2 + l^2/2} \right)^{2\alpha_P(0)} \simeq 1.88 \text{ GeV}^{-2}, \tag{20}$$

where  $M_H = 100 \text{ GeV}$  and  $s_0 - m^2 \simeq 1 \text{ GeV}^2$  is the scale parameter of the model that is used in the global fitting of the data on  $pp(p\bar{p})$  scattering for on-shell amplitudes [9]. It remains fixed in the present calculations.

If we take into account the emission of virtual ‘‘soft’’ gluons, while prohibiting the real ones, that could fill the rapidity gaps, it results in the Sudakov-like suppression [12]:

$$F_s(l^2) = \exp \left[ -\frac{3}{2\pi} \int_{l^2}^{M_H^2/4} \frac{dp_T^2}{p_T^2} \alpha_s(p_T^2) \ln \left( \frac{M_H^2}{4p_T^2} \right) \right], \tag{21}$$

and to the new value of the integral (20):

$$\begin{aligned}
I_s &\simeq \int_0^{M_H^2} \frac{dl^2}{l^4} F_s(l^2) \left( \frac{l^2}{s_0 - m^2 + l^2/2} \right)^{2\alpha_P(0)} \\
&\simeq 0.38 \text{ GeV}^{-2}, \quad M_H = 100 \text{ GeV}.
\end{aligned} \tag{22}$$

In this case the total cross-section becomes 24 times smaller than without the factor  $F_s$ .

Unitarity corrections can be estimated from the elastic  $pp$  scattering by the method depicted in Fig. 1, where

$$T_X = T_{pp \rightarrow pHp}, \tag{23}$$

$$\begin{aligned}
V(s, \mathbf{q}_T) &= 4s(2\pi)^2 \delta^2(\mathbf{q}_T) \\
&+ 4s \int d^2 \mathbf{b} e^{i\mathbf{q}_T \mathbf{b}} [e^{i\delta_{pp \rightarrow pp}} - 1], \tag{24}
\end{aligned}$$

$$\begin{aligned}
T_X^{\text{Unit.}}(p_1, p_2, \Delta_1, \Delta_2) &= \frac{1}{16ss'} \int \frac{d^2 \mathbf{q}_T}{(2\pi)^2} \frac{d^2 \mathbf{q}'_T}{(2\pi)^2} V(s, \mathbf{q}_T) \\
&\cdot T_X(p_1 - q_T, p_2 + q_T, \Delta_{1T}, \Delta_{2T}) V(s', \mathbf{q}'_T), \tag{25}
\end{aligned}$$

$$\Delta_{1T} = \Delta_1 - q_T - q'_T,$$

$$\Delta_{2T} = \Delta_2 + q_T + q'_T,$$

and  $\delta_{pp \rightarrow pp}$  can be found in [9].  $T_X$  is the ‘‘bare’’ amplitude (17), which is depicted in Fig. 2. Left and right parts  $V$  represent ‘‘soft’’ rescattering effects for initial and final states, i.e. multi-pomeron exchanges. It reduces the integrated cross-section by a factor of about 14 for the given kinematical configuration.

### 3 Results and discussions

We have the following expression for the differential cross-section:

$$\begin{aligned}
\frac{d\sigma}{dt_1 dt_2 d\xi_1 d\xi_2} &= \frac{\pi |T_{pp \rightarrow pHp}^{\text{Unit.}}|^2}{8s(2\pi)^5 \sqrt{-\lambda}}, \\
\lambda &= \kappa^2 + 2(t_1 + t_2)\kappa + (t_1 - t_2)^2 \leq 0. \tag{26}
\end{aligned}$$

By partial integrating (26) we obtain the cross-sections  $d\sigma/dt$  and  $d\sigma/d\xi$ . The first result of our calculations is depicted in Fig. 3. The antishrinkage of the diffraction peak with increasing Higgs boson mass is a direct consequence of the existence of the additional hard scale  $M_H$ , which

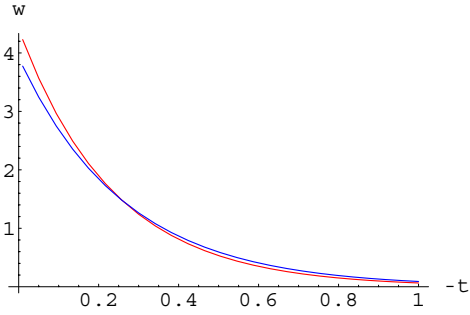


**Fig. 3.**  $t$ -distribution  $d\sigma/dt/\sigma_{\text{tot}}$  of the process  $p + p \rightarrow p + H + p$  for two different values of the Higgs boson mass

makes the interaction radius smaller. The  $\xi$  dependence is shown in Fig. 4.

The second result is the total cross-section of the EDD Higgs boson production, which can be found in Table 1 and in Figs. 5 and 6. The form of the dashed curve in Fig. 6 originates from the standard gluon–gluon–Higgs vertex and has a peak near  $M_H \simeq 2m_t$ . For the case of Sudakov-like suppression the cross-section vanishes faster with  $M_H$ .

It is useful to compare our result with other studies. Results quite close to ours (with the normalization to the CDF data,  $c_{gp} = 3.3$ ) were given in [12], where the value of the total cross-section is about 3 fb. In both cases the most important suppression in the mass region  $M_H > 100$  GeV is due to (perturbative) Sudakov factors, while the non-perturbative (absorptive) factors play a relatively minor role.

Results of other authors were considered in detail in [2]. The highest cross-section 2 pb for  $M_H = 400$  GeV at LHC energies was obtained in [6]. These authors used a non-factorized form of the amplitude and a ‘‘QCD in-

**Table 1.** Values of the total cross-section for the EDD-Higgs production

| $c_{gp}$ | $M_H$ (GeV) | $\sigma_{p+p \rightarrow p+H+p}$ (fb) |                   |
|----------|-------------|---------------------------------------|-------------------|
|          |             | LHC                                   |                   |
|          |             | no Sud. suppr.                        | Sud. suppr.       |
| 3.5      | 100 → 500   | 110 → 57                              | 4.6 → 0.14        |
| 2.3      | 100 → 500   | 20 → 11                               | –                 |
| 3.3      | 100 → 500   | –                                     | <b>3.6 → 0.11</b> |

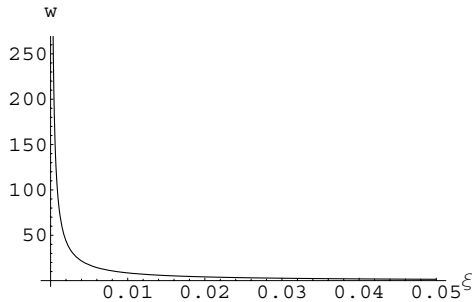


**Fig. 4.**  $\xi$ -distribution  $d\sigma/d\xi/\sigma_{\text{tot}}$  of the process  $p + p \rightarrow p + H + p$  for  $M_H = 100$  GeV

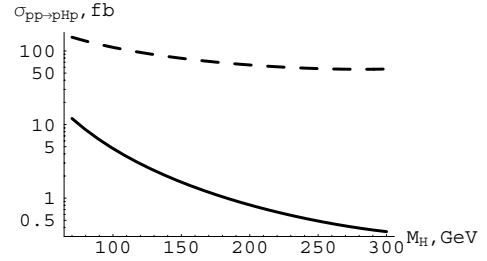


**Fig. 5.** The total cross-section (in fb) of the process  $p + p \rightarrow p + H + p$  versus Higgs boson mass for  $c_{gp} = 3.5$  without Sudakov-like suppression (dashed curve) and with Sudakov-like suppression (solid curve)

spired’’ model for  $gp \rightarrow gp$  amplitudes, taking into account the non-perturbative proton wave functions. Even if we multiply the result of [6] by the suppressing factor, it will be much larger than ours. This could serve as an indication of the possible role of non-perturbative effects. Our model is based on the Regge-eikonal approach for the amplitudes, which is primordially non-perturbative, normalized to the data from HERA on  $\gamma p \rightarrow J/\Psi p$  and improved by the CDF data on exclusive di-jet production.

To estimate the signal to QCD background ratio for the  $b\bar{b}$  signal we use the standard expression for the  $gg \rightarrow b\bar{b}$  amplitude and the following assumptions [13–16].

- (1) The possibility to separate final  $b\bar{b}$  quark jets from gluon jets. If we cannot do this, it will increase the background by two orders of magnitude. The efficiency of  $b$ -tagging is supposed to be 50%.
- (2) Suppression due to the absence of color-octet  $b\bar{b}$  final states.
- (3) Suppression of light fermion pair production, when  $J_z^{\text{tot}} = 0$  (see also [17, 18]).
- (4) The cut  $E_T > 50$  GeV ( $\theta \geq 60^\circ$ ), since the cross-section of diffractive  $b\bar{b}$  jet production strongly decreases with  $E_T$ .

The theoretical result of these numerical estimations is

$$\frac{\text{Signal}(pp \rightarrow pHp \rightarrow p\bar{b}b\bar{p})}{\text{QCD background}} \geq 9.5 \cdot 10^{-6} |f|^2 \text{Br}_{H \rightarrow Q\bar{Q}} \frac{M_H^3}{\Delta M}, \quad (27)$$

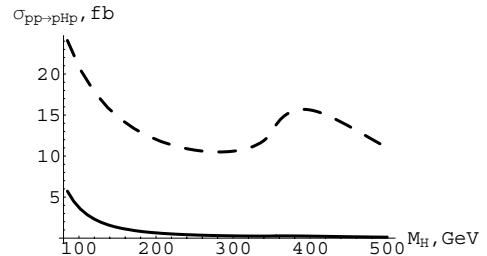


**Fig. 6.** The total cross-section (in fb) of the process  $p + p \rightarrow p + H + p$  versus Higgs boson mass for  $c_{gp} = 3.3$  with Sudakov-like suppression (solid curve) and for  $c_{gp} = 2.3$  without Sudakov-like suppression (dashed curve)

where  $|f|^2 \simeq 0.5 \rightarrow 3$  for Higgs boson masses  $100 \rightarrow 350$  GeV and numerical factor arises, when we take into account all the possible sources of the QCD background in the analogous way as in the following [14].

(1) LO backgrounds:

- (i)  $gg^{PP} \rightarrow b\bar{b}$ ,  $m_b \neq 0$ ;
- (ii)  $gg^{PP} \rightarrow gg \rightarrow "b\bar{b}"$  (1% possibility to misidentify quark jets from gluon jets);
- (iii) an admixture of  $|J_z| = 2$  production (from non-forward going protons).

(2) NLO background:  $gg^{PP} \rightarrow b\bar{b}g$ , if the extra gluon is collinear to either the  $b$  or  $\bar{b}$  jet.

Other sources are strongly suppressed. For  $M_H \simeq 115$  GeV

$$\frac{\text{Signal}(pp \rightarrow pHp \rightarrow p\bar{b}b\bar{p})}{\text{QCD background}} \geq 3.8 \frac{\text{GeV}}{\Delta M}, \quad (28)$$

where  $\Delta M$  is the mass resolution of the detector. A similar result was obtained in [13,14]. More exact estimations of the above ratio by fast Monte-Carlo simulations and the total efficiency of EDD Higgs boson production will be published in a forthcoming paper.

## 4 Conclusions

We see from the result that there is a real possibility to detect the Higgs boson using the usual  $b\bar{b}$  signal under the luminosity greater than  $10^{32}$  in EDD events at LHC. The accuracy of the mass measurements could be improved by applying the missing mass method [19].

The low value of the exclusive Higgs boson production cross-section obtained in this paper is mainly due to the Sudakov suppression factor (21), the full validity of which is not obvious for us, because the confinement effects can strongly modify the "real gluon emission".

It is interesting that in spite of different models and quite different ways of taking account of absorptive effects in our paper and in [12], the final results (see Table 1) appear to be quite close.

Certainly, the cross-sections may be larger due to still not very well known non-perturbative factors.

It is possible to generalize our approach for the exclusive production of other particles like  $\chi_{c0}$ ,  $\chi_{b0}$ , radion, KK gravitons and glueballs. In this case cross-sections can be larger than for EDD Higgs boson production, and some other important investigations like partial wave analysis and measurements of the diffractive pattern of the interaction could be done.

*Acknowledgements.* We are grateful to A. De Roeck, A. Prokudin, A. Rostovtsev, A. Sobol, S. Slabospitsky and participants of the international workshop BLOIS 2003 and several CMS meetings for helpful discussions. This work is supported by the Russian Foundation for Basic Research, grant no. 02-02-16355.

## References

1. V.A. Petrov, Proceedings of the 2nd International Symposium LHC: Physics and Detectors, by A.N. Sissakian, Y.A. Kultchitsky (eds.) June 2000, Dubna, p. 223; V.A. Petrov, A.V. Prokudin, S.M. Troshin, N.E. Tyurin, J. Phys. G Nucl. Part. Phys. **27**, 2225 (2001)
2. V.A. Khoze, A.D. Martin, M.G. Ryskin, Eur. Phys. J. C **26**, 229 (2002)
3. V.A. Petrov, Proceedings of the VIIth Blois Workshop, by M. Haguenaer et al. (eds.) Editions Frontières, Paris (1995)
4. V.A. Petrov, A.V. Prokudin, Phys. Atom. Nucl. **62**, 1562 (1999)
5. A. Kniehl, Phys. Rept. **240**, 211 (1994)
6. J.-R. Cudell, O.F. Hernandez, Nucl. Phys. B **471**, 471 (1996)
7. A. Berera, J.C. Collins, Nucl. Phys. B **474**, 183 (1996)
8. K. Goulianos, Phys. Rep. **101**, 169 (1983)
9. V.A. Petrov, A.V. Prokudin, Eur. Phys. J. C **23**, 135 (2002)
10. V.A. Petrov, A.V. Prokudin, R.A. Ryutin, hep-ph/0404116
11. CDF Collaboration (K. Borras for the collaboration), FERMILAB-CONF-00-141-E, June 2000; K. Goulianos, talk given in the Xth Blois workshop, 2003, Helsinki, Finland; M. Gallinaro, hep-ph/0311192
12. V.A. Khoze, A.D. Martin, M.G. Ryskin, Eur. Phys. J. C **14**, 525 (2000); C **21**, 99 (2001); V.A. Khoze, hep-ph/0105224
13. V.A. Khoze, A.D. Martin, M.G. Ryskin, Eur. Phys. J. C **19**, 477 (2001)
14. A. De Roeck, V.A. Khoze, A.D. Martin, R. Orava, M.G. Ryskin, Eur. Phys. J. C **25**, 391 (2002)
15. V.A. Khoze, A.D. Martin, M.G. Ryskin, Eur. Phys. J. C **23**, 311 (2002)
16. A.D. Martin, M.G. Ryskin, V.A. Khoze, Phys. Rev. D **56**, 5867 (1997)
17. A. Bialas, V. Szeremeta, Phys. Lett. B **296**, 191 (1992); A. Bialas, R. Janik, Z. Phys. C **62**, 487 (1994)
18. J. Pumplin, Phys. Rev. D **52**, 1477 (1995)
19. M.G. Albrow, A. Rostovtsev, FERMILAB-PUB-00-173 August 2000